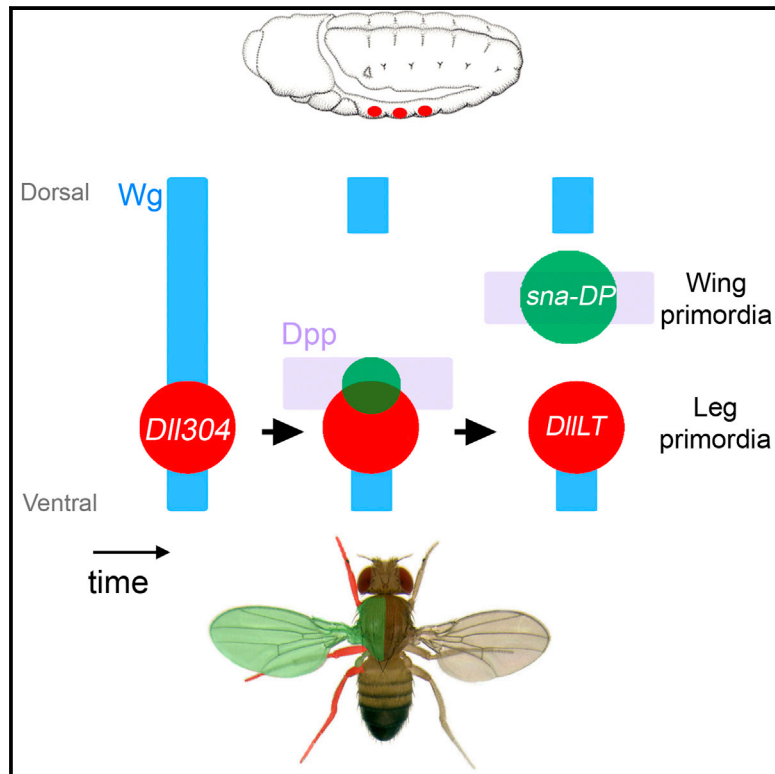


Origins and Specification of the *Drosophila* Wing

Graphical Abstract



Authors

David Requena, Jose Andres Álvarez, Hugo Gabilondo, Ryan Loker, Richard S. Mann, Carlos Estella

Correspondence

rsm10@columbia.edu (R.S.M.), cestella@cbm.csic.es (C.E.)

In Brief

By studying a *cis*-regulatory module that is specifically active in the embryonic dorsal (wing and haltere) primordia of *Drosophila*, Requena et al. demonstrate that dorsal fates are derived from two separate groups of cells, one of which shares a lineage with the ventral primordia. These data are consistent with a dual evolutionary origin of the wing.

Highlights

- An enhancer that marks the initial wing primordia in *Drosophila* is defined
- The signals that initiate wing and leg development are distinct
- Lineage experiments show that the wing comes from ventral and dorsal primordia
- Insect wings may have evolved from dual ventral and dorsal inputs

Origins and Specification of the *Drosophila* Wing

David Requena,¹ Jose Andres Álvarez,² Hugo Gabilondo,¹ Ryan Loker,³ Richard S. Mann,^{3,*} and Carlos Estella^{1,4,*}

¹Departamento de Biología Molecular and Centro de Biología Molecular Severo Ochoa, Consejo Superior de Investigaciones Científicas-Universidad Autónoma de Madrid (CSIC-UAM), Nicolás Cabrera 1, 28049 Madrid, Spain

²Departamento de Biología and Centro de Biología Molecular Severo Ochoa, Consejo Superior de Investigaciones Científicas-Universidad Autónoma de Madrid (CSIC-UAM), Nicolás Cabrera 1, 28049 Madrid, Spain

³Departments of Biochemistry and Molecular Biophysics and Systems Biology, Mortimer B. Zuckerman Mind Brain Behavior Institute, Columbia University, 701 W. 168th St., HHSC 1104, New York, NY 10032, USA

⁴Lead Contact

*Correspondence: rsm10@columbia.edu (R.S.M.), cestella@cbm.csic.es (C.E.)

<https://doi.org/10.1016/j.cub.2017.11.023>

SUMMARY

The insect wing is a key evolutionary innovation that was essential for insect diversification. Yet despite its importance, there is still debate about its evolutionary origins. Two main hypotheses have been proposed: the paranotal hypothesis, which suggests that wings evolved as an extension of the dorsal thorax, and the gill-exite hypothesis, which proposes that wings were derived from a modification of a pre-existing branch at the dorsal base (subcoxa) of the leg. Here, we address this question by studying how wing fates are initially specified during *Drosophila* embryogenesis, by characterizing a cis-regulatory module (CRM) from the *snail* (*sna*) gene, *sna*-DP (for dorsal primordia). *sna*-DP specifically marks the early primordia for both the wing and haltere, collectively referred to as the DP. We found that the inputs that activate *sna*-DP are distinct from those that activate *Distalless*, a marker for leg fates. Further, in genetic backgrounds in which the leg primordia are absent, the DP are still partially specified. However, lineage-tracing experiments demonstrate that cells from the early leg primordia contribute to both ventral and dorsal appendage fates. Together, these results suggest that the wings of *Drosophila* have a dual developmental origin: two groups of cells, one ventral and one more dorsal, give rise to the mature wing. We suggest that the dual developmental origins of the wing may be a molecular remnant of the evolutionary history of this appendage, in which cells of the subcoxa of the leg coalesced with dorsal outgrowths to evolve a dorsal appendage with motor control.

INTRODUCTION

It is estimated that nearly three-quarters of the species currently living on Earth are insects. Although there have been several hypotheses to explain this vast diversity, one likely contributing factor was the acquisition of flight due to the development of wings

approximately 350 million years ago, long before any vertebrate acquired the ability to fly [1, 2]. However, despite their importance to life on Earth, there is still debate about the evolutionary origins of insect wings [3]. One set of ideas, collectively termed the paranotal hypothesis, suggests that wings evolved as an extension from a part of the dorsal thorax called the thoracic tergum, or paranotal lobe [4, 5]. According to this hypothesis, this anatomical outgrowth initially gave insects the ability to glide, creating the opportunity for the evolution of wing anatomy and function. However, the paranotal lobe was unlikely to have any musculature or neural innervation, raising significant questions about how motor control of these dorsal outgrowths would have evolved. An alternative hypothesis proposes that wings were derived from a modification of a pre-existing branch at the dorsal base of the leg, a region referred to as the subcoxa [6–10]. In aquatic arthropods, this structure may have initially evolved as a gill, specializing in gas exchange, and subsequently modified to become a wing following terrestrialization of some crustacean lineages.

Two principal approaches have informed our current view of insect wing evolution. One approach, which depends on careful examination of the fossil record to trace the origins of the wing, has provided support for both a paranotal lobe and a subcoxa origin [5–7, 11]. One limitation of this approach is that there is a large gap in the fossil record that spans the period of time when wings first appeared. An alternative approach relies on comparing the expression patterns of molecular markers of appendages in extant insects and crustaceans that may represent the early steps of wing evolution [3]. With this approach, for example, genes that are expressed in the developing wing of *Drosophila melanogaster* were also found to be expressed in the subcoxal gills of branched appendages in two different crustaceans, consistent with a subcoxal origin for the insect wing [8, 12]. Although compelling, these types of studies also have their limitations. For one, the presence of similar markers in the fly wing and non-wing structures such as the crustacean gill could represent examples of convergent, instead of divergent, evolution. Second, many of the markers used in these studies are expressed in both leg and wing precursors, or at late stages of development, making them less definitive [13]. More recently, in two insects, wing markers were found to be expressed in two separate domains, corresponding to the positions of dorsal outgrowths and subcoxal branches, providing evidence for the idea that wings evolved from a fusion of these two initially distinct structures [3, 14, 15]. This dual-origin hypothesis

has also been supported by functional studies and recent fossil analysis [11, 16–18].

A complementary approach that may help inform the origins of insect appendages are experiments that characterize how the wing and leg primordia are initially specified during development using *cis*-regulatory modules (CRMs) that are active in the appendage primordia. Not only are these CRMs useful as markers, but they also can be used to genetically label and trace the progeny of these primordia. For example, the characterization of an early CRM from the *Distalless* (*Dll*) gene in *Drosophila*, called *Dll304*, has already provided evidence for a subcoxal origin of the wing [19, 20]. Although *Dll* function is not required for the establishment of wing fates, *Dll304* is active in a group of ~30 ventral cells early in embryogenesis, and the progeny of these cells contribute to both the ventral (leg) and dorsal (wing and haltere) appendages [20, 21]. Slightly later in embryogenesis, a different *Dll* CRM, called *DllLT*, is active in a subset of the cells that previously expressed *Dll304* [19–21]. Unlike *Dll304*, *DllLT*-expressing cells only give rise to part of the leg and do not contribute to dorsal appendages [21, 22]. In sum, these experiments reveal that *Dll*-expressing ventral cells in the early embryo contribute to both leg and wing fates, but soon thereafter, the only adult structures that *Dll*-expressing cells give rise to are legs (reviewed in [23]).

To the extent that developmental studies in extant organisms can be used to inform evolution, these findings are consistent with a shared evolutionary origin of legs and wings. However, an important but currently missing test of this idea is to characterize CRMs that are specifically active in the dorsal (wing and haltere) primordia (DP). Although several genes, including *vestigial* (*vg*), *snail* (*sna*), and *escargot* (*esg*), are well-known embryonic markers of the DP in *Drosophila*, no CRMs have yet been described that specifically label these cells [24–29]. Here, we describe the first such CRM that is specifically active in both the wing and haltere primordia during *Drosophila* embryogenesis. We use this CRM, derived from the *sna* gene, to analyze the signals and transcription factors that are required for the specification of the DP. We find that the inputs that activate this CRM are distinct from those that activate *Dll*, suggesting that the DP are, at least in part, specified independently of the ventral (leg) primordia (VP). Moreover, in genetic backgrounds in which the VP are absent or ablated, DP fates are still partially specified. Together, these results demonstrate that the dorsal appendages of *Drosophila* have a dual developmental origin: although some DP cells share a lineage with the VP, much of the DP is independently derived from non-VP cells. Based on these developmental data in *Drosophila*, we discuss the idea of a dual evolutionary origin of wings, in which cells of the sub-coxa migrated and coalesced with dorsal outgrowths to evolve a dorsal appendage with motor control.

RESULTS

Identification of the *sna*-DP CRM

The formation of the wing and haltere primordia requires the function of *sna* and *esg* [27]. Although *sna* expression is restricted to the DP, *esg* is also expressed in the VP [24–27] (Figures 1B and 2A). Therefore, we searched for CRMs of the *sna* gene specifically active in the DP.

Although multiple *sna* CRMs have been identified [30–32], none of them drive expression in the DP. An unbiased scan of the locus identified a single fragment that had such activity; notably, this fragment overlaps with VT7914 from the Vienna *Drosophila* Resource Center (VDRC) that also shows activity in the DP (Figure 1A). We named this CRM *sna*-DP and used it to drive *lacZ* reporter genes and compare its activity with *Dll* during embryonic development (Figure 1B). *sna*-DP was first detected at stage 12/13 in a few cells dorsal to *Dll*-expressing cells in the second and third thoracic segments (T2 and T3, respectively), and, by stage 14, the number of *sna*-DP cells in T2 and T3 increased to an average number of 20 and 14 cells, respectively. The *sna*-DP reporter overlaps perfectly with *Sna* and *Vg* proteins (Figure S1). Like *sna*, *sna*-DP is not active in third instar imaginal discs. However, cell-lineage tracing experiments using a minimized version of *sna*-DP (*sna*-1.7; discussed later) efficiently labeled the entire wing and haltere imaginal discs and a small number of proximal cells of all three leg discs in third instar larvae (Figures 1C and S2). Thus, *sna*-DP marks DP cells that will give rise to the dorsal regions of the T2 and T3 segments of the adult, including the wing and haltere appendages, respectively.

Partially Independent Origins of the DP and VP

Because of the shared lineages for the ventral and dorsal appendage primordia [20, 21, 33], we investigated the relationship between these primordia using *sna*-DP as a marker. First, we compared the spatial and temporal expression patterns between cells that had expressed *Dll*, using *Dll^{MD23}-Gal4*; *UAS-GFP* (*Dll*>*GFP*), and the *sna*-DP reporter (Figure 1E). The perdurance of *Gal4* and *GFP* allowed us to trace the cells that had activated, but no longer actively transcribe, *Dll*. The initial activation of *sna*-DP at stage 12/13 was observed primarily in *Dll*>*GFP* cells, while at stage 14, approximately half of the *sna*-DP-expressing cells were also labeled with *Dll*>*GFP* (Figures 1E and 1F; Movie S1), consistent with *Dll* lineage-tracing experiments (Figures 1D and S2). Although *Dll*-expressing cells can give rise to all regions of the third instar wing disc, individual wing discs are only partially labeled, and there is a bias for these cells to populate the ventral portion of the disc (Figures 1D and S2). The partial labeling of the wing discs by *Dll^{MD23}-Gal4* contrasts with near-100% labeling of the leg imaginal discs, arguing that it is unlikely due to a low efficiency of the lineage-tracing method. Curiously, lineage tracing with the early *Dll304* CRM, which is only active early and transiently, reveals a bias for labeling the anterior compartment (Figure S2).

Although these lineage-tracing experiments demonstrate that the progeny of *Dll*-expressing cells of the VP contribute to dorsal structures, they do not address whether the DP requires a contribution from the VP. We first tested this by using *Dll^{MD23}-Gal4* to ablate the ventral progenitor cells by expressing the pro-apoptotic gene *head involution defective* (*hid*). The leg and wing primordia were visualized with *esg-lacZ* (Figures 2A, 2B, and S1C). As expected, no VP cells were observed in these embryos, as seen by the absence of ventral *esg-lacZ* expression. In contrast, DP cells were still present, although the size of dorsal primordia was reduced by approximately 50% (Figure 2B). Similar results were observed when the dose of the pro-apoptotic genes was increased (Figures 2C–2E).

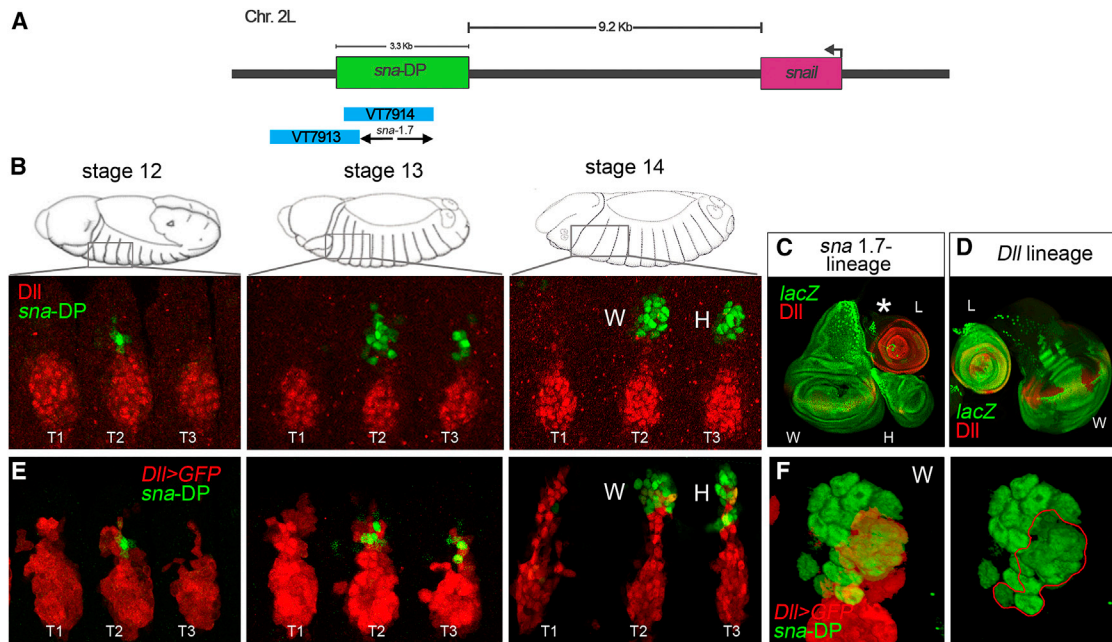


Figure 1. Overview of the *sna*-DP Enhancer and Its Relationship to *Dll* Expression

(A) The *sna* genomic region. *sna*-DP CRM (green bar) is a 3.3-kb fragment 3' to the *sna* transcription start site. VT7914, but not VT7913 (both from VDRC), is active in the DP, and *sna*-1.7 is defined by the non-overlapping region of these two fragments.
 (B) Embryonic time course of *sna*-DP activity (green) compared to *Dll* protein (red).
 (C and D) Lineage-tracing results for *sna*-DP (C) and *Dll* (D). (C) The progeny of *sna*-DP cells (green) label the entire wing and haltere imaginal discs and a small number of cells in the leg (asterisk). (D) The progeny of *Dll*-expressing cells (green) contribute to the entire leg and to parts of the wing disc (see Figure S2).
 (E) Time course of *sna*-DP activity (driving nuclear *lacZ*; green) compared to *Dll*>*GFP* (red). Note that some cells derived from the VP (due to perdurance of GFP from *Dll*>*GFP*; red) overlap with *sna*-DP-expressing DP cells (green).
 (F) An enlargement of stage 14 wing primordia.
 W, wing primordia; H, haltere primordia; L, leg primordia. See also Figures S1 and S2 and Movie S1.

We further tested the independence of the DP by examining embryos mutant for *Dll* and the ventral selector genes *button-head* (*btd*) and *Sp1* [23, 34–36]. Even in these triple-mutant embryos, *sna*-DP and *vg* were normally expressed (Figure 2G). However, although *Dll* protein was not detected, we note that *Dll*^{MD23}-*Gal4* is still active in the triple mutant, suggesting that VP fates are still partially specified (Figure S2G).

Together, these results suggest that, in the absence of the VP or when the VP is severely compromised, DP fates are still specified, although the size is reduced.

Distinct Regulation of the DP and VP

If the DP arise, in part, independently of the VP, we would expect them to have distinct genetic inputs. However, before carrying out a detailed analysis, we used both gain- and loss-of-function manipulations to demonstrate that *sna*-DP is not a *Sna*-dependent autoregulatory element and that it is activated independently of *vg*, presumably by signals and other transcription factors present in these embryos at the correct time and position (Figure S3).

Dll expression in the VP is activated by Wingless (*Wg*) and restricted dorsally and ventrally by the Decapentaplegic (*Dpp*) and epidermal growth factor receptor (EGFR) pathways, respectively [20, 37–39]. We therefore compared how these three pathways influence the formation and size of both primordia, using *sna*-DP-*lacZ* and *Dll* expression as readouts. In addition to

examining mutants, as described later, we manipulated these pathways in various ways using *prd-Gal4*, which is expressed throughout the T2, but not the T3, segment, thus allowing a comparison of *prd-Gal4*-expressing and non-expressing segments in the same embryo (Figure S3).

Wg

Initially, *wg* is expressed in dorso-ventral stripes in the anterior compartment of each thoracic segment that are later interrupted due to repression by the T-box transcription factors encoded by the three *Dorsocross* (*Doc*) genes [40]. Repression of *wg* by *Doc* creates a *Wg*-free domain in the lateral ectoderm (Figures 3A–3C). *sna*-DP activity is only observed after *wg* repression and within the *Doc* expression domain (Figures 3D–3F). Consistent with these expression patterns, ectopic activation of the *Wg* pathway by expressing an activated form of the transcriptional co-activator Armadillo (*Arm*^{*}) results in smaller DP and an increase in the number of VP cells (Figures 4C and 4O). Conversely, downregulation of the *Wg* pathway using a dominant-negative version of the *Wg* transcriptional effector TCF (TCF^{DN}) had no effect on *sna*-DP but completely abolished *Dll* expression (Figures 4B and 4O). Moreover, in embryos homozygous for a deficiency that removes all three *Doc* genes, *Df(3L)DocA*, the DP are absent, and there is a dramatic expansion of the *Dll*-expressing VP (Figures 4D and 4O). Ectopic expression of one of the *Doc* genes, *Doc-2*, eliminates the VP, while the number of *sna*-DP-positive cells remains

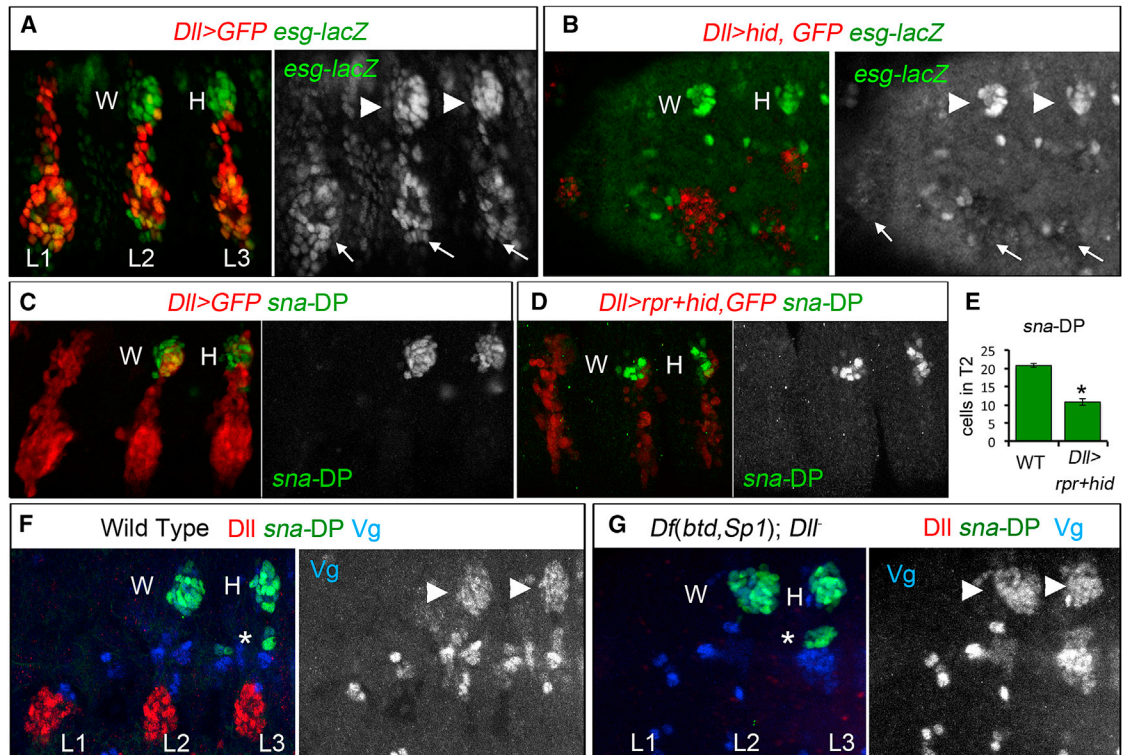


Figure 2. The DP Is Reduced when the VP Is Ablated

(A) Thoracic view of *esg-lacZ* (green) and *Dll>GFP* (red) expression in WT stage 14 embryos. The three legs and DP are labeled with arrows and arrowheads, respectively.
 (B) Genetic ablation of the VP in *Dll>hid* embryos (red and arrows) reduced the size of the DP (arrowheads) and eliminates ventral expression of *esg-lacZ* (arrows).
 (C) Thoracic view of *sna-DP* (green) and *Dll>GFP* (red) in WT stage 14 embryo.
 (D) Ablation of the VP in *Dll>rpr+hid* embryos (red) reduced the size of the DP (green).
 (E) Quantification of the number in T2 of *sna-DP* (green bars) in WT and *Dll>rpr+hid* embryos. * $p < 0.05$ with Student's t test. Error bars represent SEM.
 (F) WT stage 14 embryo stained for *sna-DP-lacZ* (green), Vg (blue), and Dll (red).
 (G) A stage 14 *Df(btd,Sp1); Dll* embryo. DP size is unaffected.
 An asterisk in (F) and (G) labels a band of muscle cells that express *sna-DP* and Vg. W, wing primordia; H, haltere primordia; L, leg primordia. See also Figure S2.

unchanged (Figures 4E and 4O). These data are consistent with the idea that Doc-mediated repression of *wg* is necessary for the formation of the DP and that *wg* is an essential activator of the VP [20, 39, 41].

Dpp

The dorsal and ventral appendage primordia also have different responses to *dpp*, which is initially expressed as a dorsal spot within *Dll*-expressing cells and gradually expands dorsally along with *sna-1.7* activity (minimized version of *sna-DP*) (Figures 3G–3I). The expression of a constitutively active version of the Dpp receptor, *thickveins^{OD}* (*tkv^{OD}*) almost doubles the size of the DP without affecting the size of the VP (Figures 4G and 4O). Inhibition of the Dpp pathway through the expression of the Dpp pathway repressor Brinker (Brk) abolishes both *sna-DP* and *Dll* expression (Figures 4F and 4O). The effects of Dpp manipulations on *sna-DP* are consistent with previous findings that *dpp* is required for Doc expression [40, 41].

EGFR

Activation of the EGFR pathway, as visualized using an antibody to phospho-MAP kinase (pMAPK), is initially detected in *Dll*-expressing cells at stage 10/11, and by stage 14, it is restricted to a subset of the VP and is mostly absent from the DP (Figures

3J–3L). Consistent with previous results [38], in *EGFR* mutant embryos, the size of the DP increases while the size of the VP is reduced (Figures 4H and 4O). Conversely, expression of a constitutively active version of the EGFR receptor (*EGFR.λtop*) reduces the size of the DP and increases the size of the VP (Figures 4I and 4O).

Epistasis Experiments

The experiments described earlier suggest that the activation of the Doc genes by Dpp results in the repression of *wg* in the lateral ectoderm, thus generating a permissive domain where *sna-DP* can be activated. To further investigate the roles of Dpp, Doc, and Wg, we carried out epistasis experiments to more precisely decipher the logic of *sna-DP* activation.

Initially, we tested whether the activation of the Dpp pathway, which increases the size of the DP, would increase their size further when the Wg pathway was downregulated. In *prd>tkv^{OD}*, *TCF^{DN}* embryos, the size of the DP increased compared to that of wild-type (WT) (compare Figure 4J with 4A) but was similar to the size observed in *prd>tkv^{OD}* embryos (compare Figure 4J with 4G and 4O).

We next asked whether the Doc genes play a role in *sna-DP* activation besides its indirect role through the repression of *wg*.

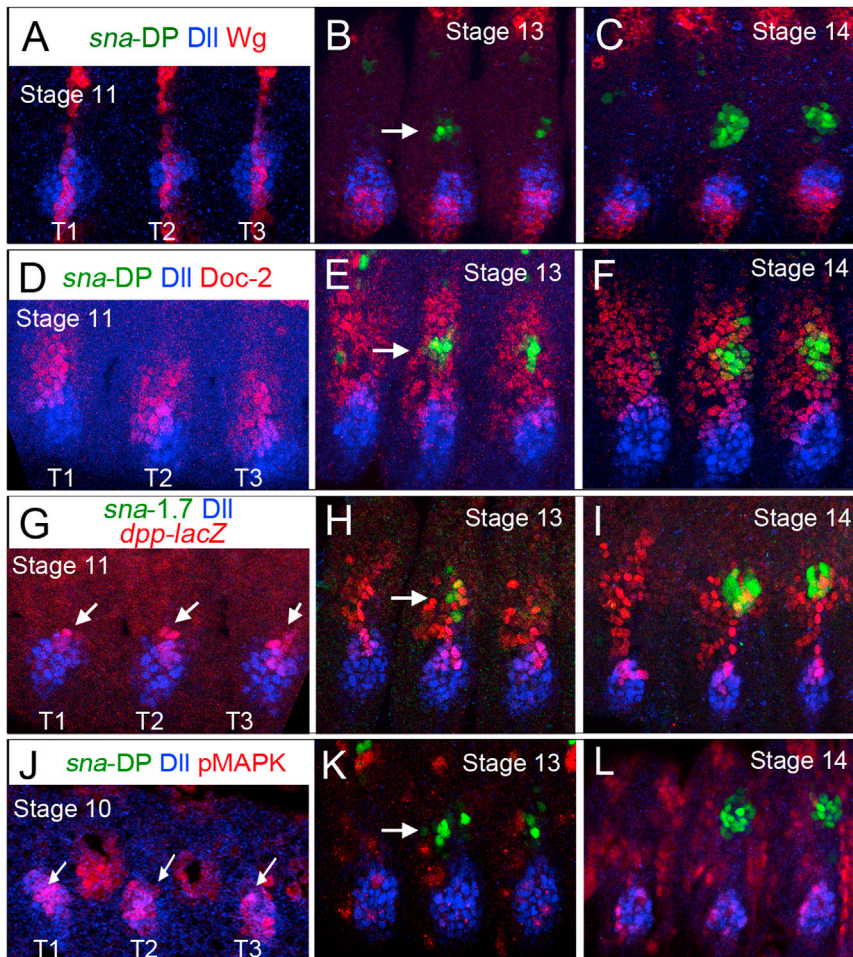


Figure 3. Relationship between *sna*-DP, *Dll*, *Doc*, and Signaling Pathways

All panels show thoracic views of WT embryos stained for the indicated markers. See also Figure S3.

(A–C) At stage 11 (A), *Wg* is expressed in uninterrupted dorso-ventral stripes. Later, *sna*-DP is activated in a lateral domain where the *Wg* stripe is interrupted (arrow). (B) Stage 13. (C) Stage 14.

(D–F) *sna*-DP is activated within the *Doc*-2 domain (arrow). (D) Stage 11. (E) Stage 13. (F) Stage 14. (G–I) *dpp* is initially expressed as a dorsal spot within *Dll*-expressing cells (arrows). (G) Stage 11. At (H) stage 13 and (I) stage 14; *sna*-DP is activated in *dpp-lacZ*-expressing cells.

(J–L) pMAPK is detected within *Dll*-expressing cells at (J) stage 10 (arrows). *sna*-DP is active in cells with low or no pMAPK staining. (K) Stage 13. (L) Stage 14.

Hox Regulation of *sna*-DP

Although the *Wg*, *Dpp*, and EGFR pathways are deployed similarly in all thoracic and abdominal segments of the embryo, the DP are only formed in the T2 (wing) and T3 (halter) segments (Figure 1B). Previous results suggest that the Hox proteins control the segmental expression of *Dll* and *vg* [19, 29], and, for *Dll*, direct Hox inputs have been defined that restrict its expression to the three thoracic segments [19, 42, 43]. To investigate the relationship between the Hox genes and the DP, we first compared the

First, we tried to rescue the lack of *sna*-DP activation in *tkv^{a12}* null mutant embryos by expressing *Doc*-2 with *prd-Gal4*. *Doc*-2 was not sufficient to induce *sna*-DP in the absence of *tkv*, suggesting a *Doc*-independent role for the *Dpp* pathway in activating *sna*-DP (Figure 4K). Similarly, *sna*-DP expression was not rescued in *Df(3L)DocA* embryos in which the *Wg* pathway was downregulated by the expression of *TCF^{DN}*, suggesting that *Doc* plays a positive role in addition to the repression of *wg* (Figure 4L). In a third experiment, we examined *Df(3L)DocA* embryos in which the *Dpp* pathway was also upregulated. In these embryos, we observed a small number of *sna*-DP-positive cells dorsal to the *Dll* domain (Figure 4M). This limited rescue could be due to ectopic expression of *wg* typical of *Df(3L)DocA* mutant embryos [40]. To test for this, we also downregulated the *Wg* pathway in these embryos (*Df(3L)DocA*; *prd>tkv^{AD}*, *TCF^{DN}*). In these embryos, activation of the *Dpp* pathway was sufficient to increase the number of *sna*-DP-expressing cells (Figure 4N).

Together, these epistasis experiments indicate that *sna*-DP is activated by the *Dpp* pathway by two parallel mechanisms: one is via *Dpp*'s activation of *Doc* (which represses *wg*), and one is independent of *Doc* (Figure 7). We further conclude that the primary role for *Doc* in the activation of *sna*-DP is to repress *wg*.

expression of the Hox genes *Scr*, *Antp*, *Ubx*, and *abd-A* with *sna*-DP (Figures 5A–5D). At the stage when *sna*-DP is fully activated in T2 and T3 (stage 14), *Scr* is restricted to the first thoracic segment, T1 (Figure 5A). *Antp* protein is observed in all three thoracic segments, where it overlaps with *sna*-DP at stage 13 (Figure S4). However, by stage 14, *Antp* is not observed in *sna*-DP-positive cells (Figure 5B). In contrast, *Ubx* overlaps with *sna*-DP in the haltere primordia in T3 but not with the wing primordia in T2 (Figure 5C). *Abd-A* is restricted to the abdominal segments, with higher levels in the posterior compartment (Figure 5D).

As the regulation of the VP gene *Dll* is compartment specific [43], we examined the relationship between *sna*-DP and the posterior-compartment gene *engrailed* (*en*) in WT and Hox mutant embryos. In *Scr* mutant embryos, ectopic DP are observed in the T1 segment, in both anterior and posterior compartments (Figure 5F). In *Antp* mutants, *sna*-DP is expressed in both compartments, but the number of cells is reduced in T2 (Figures 5G and 5Q). In *Ubx* mutant embryos, *sna*-DP is derepressed in the anterior compartment of the first abdominal segment (A1) (Figures 5H and 5Q). Consistent with this observation, in *abd-A* mutant embryos, *sna*-DP is derepressed in ~4 posterior-compartment cells in abdominal segments (Figure 5I), and in *Ubx abd-A* double-mutant embryos, *sna*-DP is derepressed

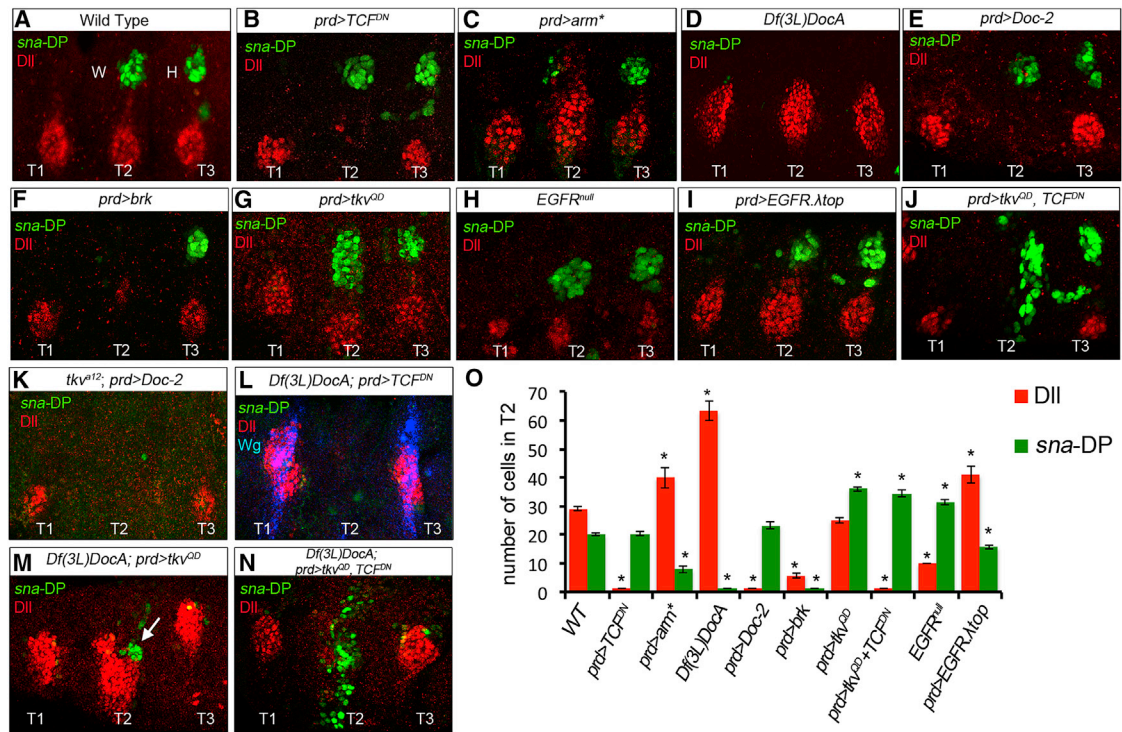


Figure 4. Distinct Regulation of *Dll* and *sna-DP*

Thoracic regions of stage 14 embryos stained for *Dll* (red) to mark the VP, *sna-DP* (green), to mark the DP, and Wg (blue) in (L).

(A) WT.

(B) In *prd>TCF^{DN}* embryos, the VP are absent and DP are not affected in T2.

(C) In *prd>arm^{*}* embryos, VP size increases and DP size decreases in T2.

(D) In *Df(3L)DocA* embryos, DP are absent and VP size is doubled.

(E) In *prd>Doc-2* embryos, VP are absent and DP size is unchanged.

(F) In *prd>brk* embryos, both the VP and DP are absent in T2.

(G) In *prd>tkv^{OD}* embryos, DP size increases, while VP size is unchanged in T2.

(H) In *EGFR^{null}* mutant embryos, VP size is reduced and DP size increases.

(I) In *prd>EGFR.λtop* embryos, VP size increases and DP size is reduced in T2.

(J) In *prd>tkv^{OD}, TCF^{DN}* embryos, DP size increases and shifts them ventrally, VP are absent.

(K) A *tkv^{at12}, prd>Doc-2* embryo. Without Dpp signaling, resupplying *Doc-2* does not rescue DP formation.

(L) A *Df(3L)DocA, prd>TCF^{DN}* embryo. Reducing Wg pathway activation in the absence of the *Doc* genes fails to rescue DP formation. *Dll* and *wg* expression are absent in T2.

(M) A *Df(3L)DocA, prd>tkv^{OD}* embryo. Increasing Dpp pathway activity partially rescues DP formation (arrow).

(N) A *Df(3L)DocA; prd>tkv^{OD}, TCF^{DN}* embryo. Simultaneously activating the Dpp pathway and repressing the Wg pathway in the absence of the *Doc* genes further increases DP size (compare with M).

(O) Quantification of DP (green bars) and VP (red bars) size in the genetic backgrounds shown in (A)–(J). **p* < 0.05, with Student's *t* test, indicating a significant difference from WT T2. Error bars represent SEM.

in both anterior- and posterior-compartment cells of the abdominal segments (Figure 5J). In *Ubx* and *Ubx abdA* mutant embryos, we also noticed a reduction in the number of *sna-DP* cells in T2 compared to WT embryos, which may be a consequence of partial derepression of *Scr* (Figures 5Q and S4).

Ectopic expression experiments, using the *prd-Gal4* driver, were also informative (Figures 5K–5P). *prd>Scr* is able to nearly eliminate both *sna-DP* and *Dll*, while expressing *abd-A* or *Abd-B* completely eliminates both primordia. In contrast, although *prd>Ubx* fully eliminates the VP, it only reduces the size of the DP. *prd>Antp* did not have any noticeable effect on either *Dll* or *sna-DP*. Finally, because a portion of the DP is derived from the VP, we considered the possibility that Hox repression of the DP could, in part, be an indirect consequence of VP

repression. However, by using a *Gal4* driver that is active in dorsal, but not ventral, regions of each segment, to drive the expression of abdominal Hox proteins, we found that they can repress the DP independently of the VP (Figure S5).

Molecular Dissection of *sna-DP*

To address how the signals that regulate the expression of *sna* are integrated at a molecular level, we further dissected the *sna-DP* CRM. We reduced the original *sna-DP* to a 1.7-kb fragment (*sna-1.7*) by comparison to other reporter lines (Figure 1A; STAR Methods). Next, we subdivided the *sna-1.7* CRM into 4 overlapping fragments (Figures 6A and 6B). Although the background of *lacZ* increased after minimizing the *sna-1.7* fragment, the activity in the DP stands out, compared to the background.

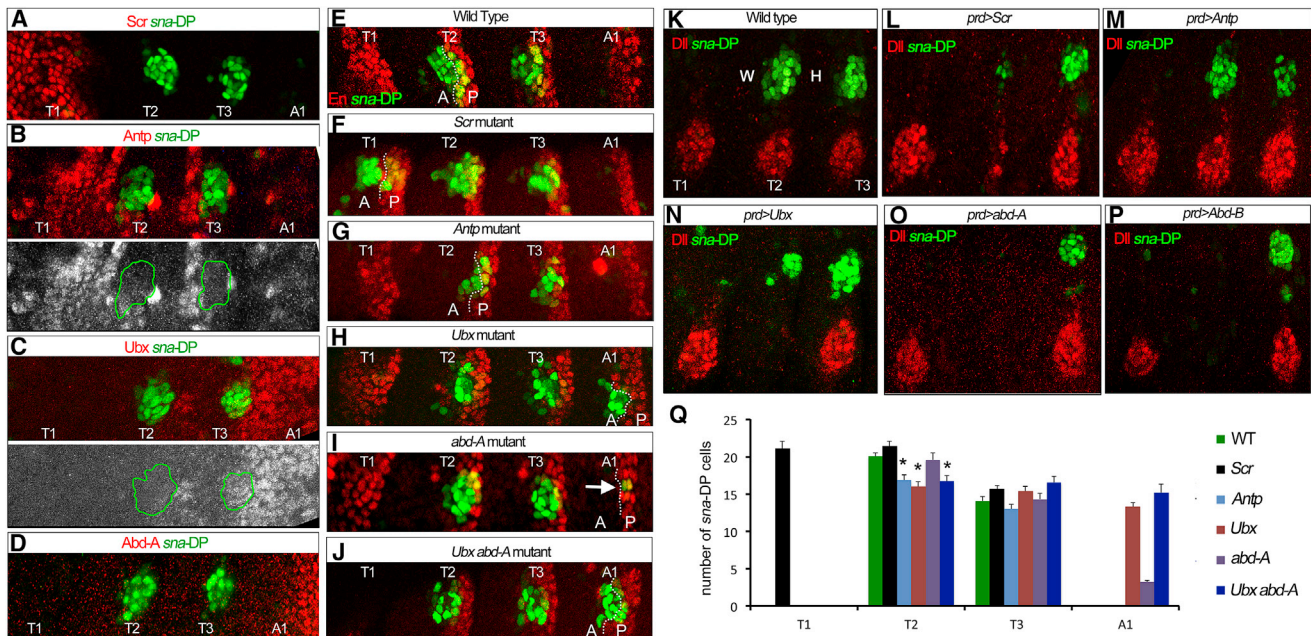


Figure 5. Hox Regulation of *sna*-DP

(A–D) Thoracic and first abdominal segments of stage 14 embryos stained for *sna*-DP (green) and Scr (red in A), Antp (red or white in B), Ubx (red or white in C) and Abd-A (red in D). The wing and haltere primordia are outlined in green.

(E–J) Thoracic and first abdominal segments of stage 14 embryos stained for *sna*-DP (green) and En (red) in WT (E), *Scr* (F), *Antp* (G), *Ubx* (H), *abd-A* (I), and *Ubx abd-A* (J) double-mutant embryos. The anterior (A)-posterior (P) compartment border is indicated with a dotted line. Arrow in (H) points to *sna*-DP cells in the P compartment of A1 in *abdA* mutant embryos.

(K–P) Thoracic segments of stage 14 embryos stained for *sna*-DP (green) and *Dll* (red) in WT (K), *prd>Scr* (L), *prd>Antp* (M), *prd>Ubx* (N), *prd>abd-A* (O), and *prd>Abd-B* (P) embryos. Ectopic expression of *Scr*, *abd-A*, or *Abd-B* in T2 represses *Dll* and *sna*-DP, while *prd>Antp* does not change these readouts. *prd>Ubx* reduces the size of the DP domain and eliminates *Dll*.

(Q) Quantification of DP size in T2 in Hox mutant genotypes. **p* < 0.05, with Student's t test, indicating a significant difference from WT T2. Error bars represent SEM. See also Figures S4 and S5.

Only the *sna*-1.7-2 fragment reproduced the expression of *sna* in both the anterior and posterior compartments of the DP (Figure 6B). *sna*-1.7-3 activity was mostly restricted to the posterior compartment (Figure 6B) but can eventually contribute to both compartments when tested in lineage-tracing experiments (Figure S2). Further attempts to dissect *sna*-1.7-2 into smaller subfragments (*sna*-1.7-2A and *sna*-1.7-2.B) were unsuccessful, suggesting that both halves are required for activity (Figure S6). Notably, when in *trans* to an intact *sna*-1.7 reporter inserted into the same chromosomal location, the activity of these subfragments was rescued, most likely by a phenomenon known as transvection [44] (Figure S6).

Because of Dpp's positive role in *sna* activation, we searched for binding sites of the transcription factor Mothers against Dpp (Mad) within the minimal *sna*-1.7-2. We found 3 predicted sites that when mutated (*sna*-1.7-2^{Mad}) strongly reduced the levels of the reporter gene expression (Figures 6E and S6). We also identified a site that binds Antp together with the Hox cofactors Extradenticle (Exd) and Homothorax (Hth) that, when mutated, reduced expression (*sna*-1.7-2^{Hox1Δ2}) (Figures 6F and S7). However, mutation of this or other putative Hox-binding sites failed to result in derepression in the abdominal or T1 segments, leaving open the question of whether Hox repression of *sna*-DP in these segments is direct (Figures 6F and 6G).

DISCUSSION

Here, we describe the first CRM in *Drosophila*, *sna*-DP, that is specifically active in the embryonic progenitors of the wing and haltere imaginal discs. Lineage-tracing experiments using this element demonstrate that the embryonic cells marked by *sna*-DP are the progenitors for the entire adult thorax of segments T2 and T3, not just the dorsal appendages (wing and haltere). Thus, by comparing the regulation of *sna*-DP to that of VP-restricted genes and CRMs, we have been able to unambiguously compare the genetic inputs that specify these two primordia, as well as their lineages and spatial relationship to each other. In the following text, we discuss these findings and how they help inform the evolutionary origins of the wing.

Different Inputs for Specifying the VP and DP

Using *Dll* and a *sna*-DP reporter gene as readouts, we extend previous findings to derive the regulatory inputs into the initial specification of these two primordia [19–21, 29, 37–39, 42, 43]. Our key findings, combined with previous observations, are summarized in Figure 7. In stage 11 embryos, *Dll* is first activated in a group of ~30 cells in each thoracic segment in a Wg-dependent manner. Because these cells can give rise to both ventral and dorsal structures, we refer to this group of cells as the thoracic primordia (TP), to highlight the fact that they have a broader

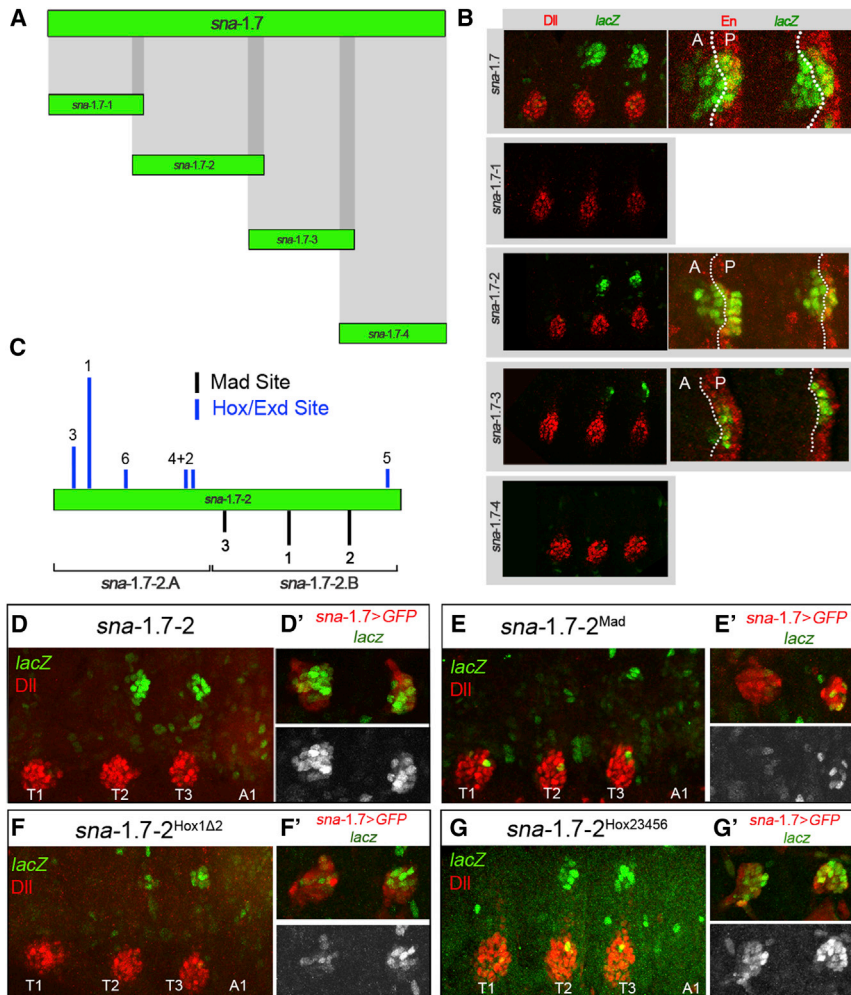


Figure 6. Molecular Dissection of *sna*-DP

(A) Division of *sna-1.7* into 4 overlapping fragments.

(B) Thoracic segments of stage 14 embryos stained for *Dll* or *En* (red) and β -galactosidase (*lacZ*, green). *sna-1.7* reproduces the activity of *sna*-DP in both the anterior (A) and posterior (P) compartments. *sna-1.7-2* is active in both compartments, while *sna-1.7-3* is mostly restricted to the P compartment. *sna-1.7-1* and *sna-1.7-4* do not drive any expression in the DP.

(C) *sna-1.7-2* has predicted binding sites for Hox/Exd (blue lines) and Mad (black lines). The height of the bar indicates the relative score (JASPAR). Subfragments *sna-1.7-2.A* and *sna-1.7-2.B* are indicated.

(D–G) Thoracic and first abdominal segments of stage 14 embryos stained for *Dll* (red) and β gal (green). The right panels show the region of the DP where the activity of *sna-1.7>GFP* (red) is compared to the activity of mutant *sna-1.7-2* elements (green or white). (D) *sna-1.7-2*. (E) *sna-1.7-2^{Mad}* with the three predicted Mad sites mutated. (F) *sna-1.7-2^{Hox1Δ2}* with Hox site 1 mutated. (G) *sna-1.7-2^{Hox23456}* with Hox sites 2–6 mutated.

See also Figures S6 and S7.

developmental potential compared to the VP, which is defined by the set of *Dll*-expressing cells a few hours later. At this initial stage, the size of the TP is restricted by EGFR ventrally and *Dpp* dorsally [20, 37]. Also at this early stage, *Wg* is expressed in a continuous stripe along the dorsal-ventral axis. Soon thereafter, expression of the *Doc* genes is activated in a set of lateral cells in a *Dpp*-dependent manner [41] and is responsible for repressing *wg*, thus interrupting the *Wg* stripe [40]. Our experiments demonstrate that both conditions—an absence of *Wg* and presence of *Dpp*—are required for the initial expression of *sna*-DP, which is activated in the *Dpp*- and *Doc*-expressing and *Wg*-non-expressing region of the embryo. The identification of essential Mad-binding sites suggests that the activation of *sna*-DP by *Dpp* is direct. In contrast to *Dpp* activation of the DP, the primary inducer of *Dll* in the VP is *Wg* [21, 22, 39]. The role of EGFR signaling is more complex: although it is initially required to restrict *Dll* expression from the ventral midline, this expansion of *Dll* is likely because of a transformation of cell fate [37]. Later in embryogenesis, EGFR signaling plays an activating role in specifying the VP and a negative role in specifying the DP, consistent with previous observations [38].

The TP and, subsequently, the VP are not present in abdominal segments due to repression by the abdominal Hox proteins

expressing cells in *Antp* null embryos. Interestingly, *Antp* has recently been shown to have a positive role in VP size [45]. Further, as observed for *Dll* [43], repression of *sna*-DP by the abdominal Hox proteins occurs in a compartment-specific manner. We also found that a subfragment of *sna*-DP (*sna-1.7-3*) is mostly expressed in the posterior compartment of T2 and T3, suggesting that the compartment-specific repression by *Ubx* and *Abd-A* is mediated by distinct inputs into *sna*-DP. However, unlike the regulation of *Dll* in the VP, we have been unable to separate the positive (by *Antp*) and negative (by *Scr*, *Ubx*, and *Abd-A*) Hox inputs into *sna*-DP: when Hox-binding sites in *sna*-DP were mutated, we only observed reduced expression, thereby leaving unresolved the question of whether Hox-mediated abdominal repression of *sna*-DP is direct. Further, we note that assessing *Ubx*'s role in T3 is not straightforward: while the size of the DP is smaller in T3 compared to that in T2, in *Ubx* null embryos, DP size in T3 does not change. This may, in part, be because of derepression of *Scr*, which could limit our ability to observe the expected increase in DP size in *Ubx* null embryos. Nevertheless, ectopic expression of *abd-A* in T2 completely eliminates the DP, while ectopic expression of *Ubx* in T2 only reduces the size of DP, highlighting an interesting difference between the activities of these two abdominal Hox proteins.

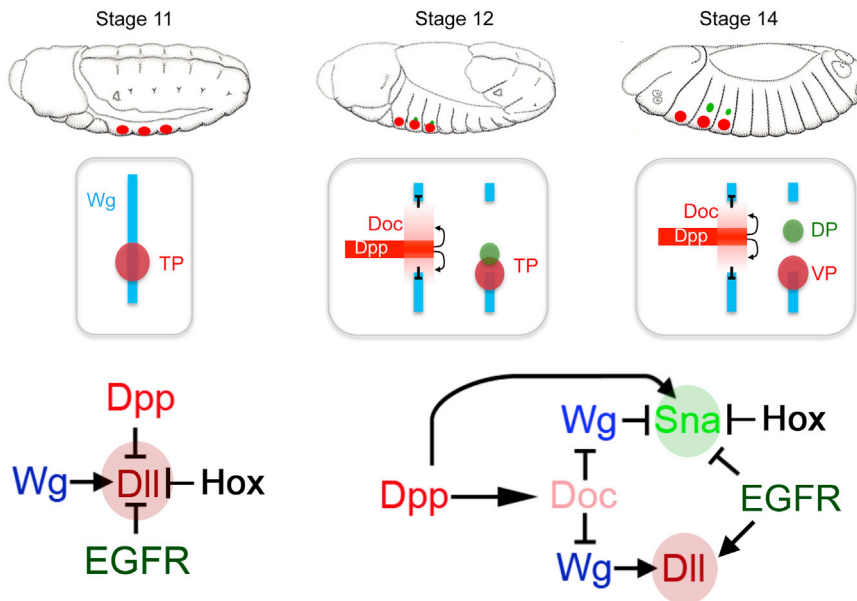


Figure 7. Origin and Specification of the *Drosophila* Wing

At stage 11, *wg* is expressed in continuous dorso-ventral stripes in each segment of the embryo. As the initial group of *Dll*-expressing cells (red circles) contributes to both the DP and VP, we refer to them as thoracic primordia (TP). By stage 12, *Doc* is activated by *Dpp* and represses *wg* in the lateral ectoderm. The dorsal primordia (DP, green circle) originate from two populations of cells: one within the TP (cells that had previously expressed *Dll*) and a second group dorsal to the TP. As embryogenesis progresses, the DP separates from the VP. The bottom panels show the known inputs into *Dll* and *sna*-DP when *Dll* is first activated (left) and when *sna*-DP is activated (right).

Implications for the Evolution of Wings

Our lineage-tracing data demonstrate that the wing and haltere imaginal discs are derived from two populations of cells: those that originate in the TP (marked by activity of the early *Dll* CRM, *Dll304*) and those that receive distinct cues (high *Dpp*, low *Wg*) in more dorsal positions of the thoracic segments. Although these lineage-tracing experiments suggest that both populations of cells have the potential to give rise to any part of the wing and haltere imaginal discs, we highlight two differences. First, lineage tracing using TP drivers labels only a portion of each wing disc, and the labeled cells have a tendency to be in the ventral portion of the disc. The ventral bias may be a consequence of the ventral position of the TP relative to the DP, suggesting that the fate of these cells is due to their relative position in the embryo. In contrast, lineage tracing performed with *sna*-DP is 100% efficient, consistently labeling the entire wing and haltere imaginal discs. The complete labeling of these discs by *sna*-1.7 argues that the cells that express that CRM, which include the cells derived from the TP, are the precursors of the entire dorsal thorax.

We suggest that the dual developmental origins of the wing primordia may be a molecular remnant of the evolutionary history of this appendage and, thus, support a dual evolutionary origin of the wing. Interestingly, this idea has also been suggested based on recent expression studies of wing marker genes [3, 14, 15], functional approaches [16, 17], and fossil analysis [18]. In future work, it will be interesting to investigate whether similar CRMs with *sna*-DP-like activity are conserved in other organisms such as crustaceans. Interestingly, and consistent with this notion, it is noteworthy that a *sna* ortholog is expressed adjacent to the limb buds in the crustacean *Parhyale hawaiiensis* [46].

In summary, by carrying out CRM-based lineage analyses and genetic studies, our observations complement comparative expression approaches and provide additional support for a dual-origin model of the dorsal appendages. From an

evolutionary point of view, there are two advantages of such a model. For one, the dorsal contribution to the wing could have provided an initial wing-like structure that allowed airborne insects to glide. Second, a ventral/coxa contribution could have provided an initial source of muscles innervated by motor neurons, allowing directed movements of this structure. It is particularly striking that the dual origins of the DP are still observable in a dipteran fly such as *Drosophila*, which, unlike crustaceans, undergoes holometabolism development where the adult structures develop from cells set aside early in embryogenesis. If the dual specification of the dorsal appendage occurs in both holo- and hemimetabolism insects, it would support the idea that it predates the origin of holometabolism.

evolutionary point of view, there are two advantages of such a model. For one, the dorsal contribution to the wing could have provided an initial wing-like structure that allowed airborne insects to glide. Second, a ventral/coxa contribution could have provided an initial source of muscles innervated by motor neurons, allowing directed movements of this structure. It is particularly striking that the dual origins of the DP are still observable in a dipteran fly such as *Drosophila*, which, unlike crustaceans, undergoes holometabolism development where the adult structures develop from cells set aside early in embryogenesis. If the dual specification of the dorsal appendage occurs in both holo- and hemimetabolism insects, it would support the idea that it predates the origin of holometabolism.

STAR★METHODS

Detailed methods are provided in the online version of this paper and include the following:

- KEY RESOURCES TABLE
- CONTACT FOR REAGENTS AND RESOURCE SHARING
- EXPERIMENTAL MODEL AND SUBJECT DETAILS
 - Fly and embryo culture
 - Fly stocks
- METHOD DETAILS
 - Immunofluorescence
 - Generation of transgenes
 - Electrophoretic mobility shift assays (EMSAs)
- QUANTIFICATION AND STATISTICAL ANALYSIS

SUPPLEMENTAL INFORMATION

Supplemental Information includes seven figures and one movie and can be found with this article online at <https://doi.org/10.1016/j.cub.2017.11.023>.

AUTHOR CONTRIBUTIONS

D.R., J.A.A., H.G., R.L., and C.E. performed the experiments. D.R., J.A.A., H.G., R.L., C.E., and R.S.M. analyzed the data. C.E. and R.S.M. wrote the manuscript.

ACKNOWLEDGMENTS

We thank Ingolf Reim, Ernesto Sánchez-Herrero, and Fernando Diaz-Benjumea for fly stocks and reagents. We thank Richard Allan for his initial contributions to the project and Nuria Esteban for technical help. We also thank Ernesto Sánchez-Herrero, Molly Przeworski, and members of the Mann and Estella labs for comments on the manuscript. This study was supported by grants from the Secretaría de Estado de Investigación, Desarrollo e Innovación (Ministerio de Economía y Competitividad) (BFU2015-65728-P to C.E.) and NIH grants RO1GM058575 and R35GM118336 to R.S.M.

Received: June 19, 2017

Revised: October 11, 2017

Accepted: November 8, 2017

Published: December 7, 2017

REFERENCES

- Engel, M.S. (2015). Insect evolution. *Curr. Biol.* **25**, R868–R872.
- Grimaldi, D., and Engel, M. (2005). *Evolution of the Insects* (Cambridge University Press).
- Clark-Hachtel, C.M., and Tomoyasu, Y. (2016). Exploring the origin of insect wings from an evo-devo perspective. *Curr. Opin. Insect Sci.* **13**, 77–85.
- Snodgrass, R.E. (1935). *Principles of Insect Morphology* (McGraw-Hill).
- Crampton, G.C. (1916). Phylogenetic origin and the nature of the wings of insects according to the paranotal theory. *J. N.Y. Entomol. Soc.* **24**, 1–39.
- Kukalova-Peck, J. (1983). Origin of the insect wing and wing articulation from the arthropodan leg. *Can. J. Zool.* **61**, 1618–1669.
- Kukalova-Peck, J. (1978). Origin and evolution of insect wings and their relation to metamorphosis, as documented by the fossil record. *J. Morphol.* **156**, 53–125.
- Averof, M., and Cohen, S.M. (1997). Evolutionary origin of insect wings from ancestral gills. *Nature* **385**, 627–630.
- Wigglesworth, V. (1973). Evolution of insect wings and flight. *Nature* **246**, 127–129.
- Coulcher, J.F., Edgecombe, G.D., and Telford, M.J. (2015). Molecular developmental evidence for a subcoxal origin of pleurites in insects and identity of the subcoxa in the gnathal appendages. *Sci. Rep.* **5**, 15757.
- Rasnitsyn, A. (1981). A modified paranotal theory of insect wing origin. *J. Morphol.* **168**, 331–338.
- Damen, W.G., Saridakis, T., and Averof, M. (2002). Diverse adaptations of an ancestral gill: a common evolutionary origin for wings, breathing organs, and spinnerets. *Curr. Biol.* **12**, 1711–1716.
- Jockusch, E.L., and Nagy, L.M. (1997). Insect evolution: how did insect wings originate? *Curr. Biol.* **7**, R358–R361.
- Clark-Hachtel, C.M., Linz, D.M., and Tomoyasu, Y. (2013). Insights into insect wing origin provided by functional analysis of vestigial in the red flour beetle, *Tribolium castaneum*. *Proc. Natl. Acad. Sci. USA* **110**, 16951–16956.
- Niwa, N., Akimoto-Kato, A., Niimi, T., Tojo, K., Machida, R., and Hayashi, S. (2010). Evolutionary origin of the insect wing via integration of two developmental modules. *Evol. Dev.* **12**, 168–176.
- Elias-Neto, M., and Belles, X. (2016). Tergal and pleural structures contribute to the formation of ectopic prothoracic wings in cockroaches. *R. Soc. Open Sci.* **3**, 160347.
- Medved, V., Marden, J.H., Fescemyer, H.W., Der, J.P., Liu, J., Mahfooz, N., and Popadić, A. (2015). Origin and diversification of wings: insights from a neopteran insect. *Proc. Natl. Acad. Sci. USA* **112**, 15946–15951.
- Prokop, J., Pecharová, M., Nel, A., Hörschemeyer, T., Krzemińska, E., Krzemiński, W., and Engel, M.S. (2017). Paleozoic nymphal wing pads support dual model of insect wing origins. *Curr. Biol.* **27**, 263–269.
- Vachon, G., Cohen, B., Pfeifle, C., McGuffin, M.E., Botas, J., and Cohen, S.M. (1992). Homeotic genes of the bithorax complex repress limb development in the abdomen of the *Drosophila* embryo through the target gene *Distal-less*. *Cell* **71**, 437–450.
- Cohen, B., Simcox, A.A., and Cohen, S.M. (1993). Allocation of the thoracic imaginal primordia in the *Drosophila* embryo. *Development* **117**, 597–608.
- McKay, D.J., Estella, C., and Mann, R.S. (2009). The origins of the *Drosophila* leg revealed by the cis-regulatory architecture of the *Distalless* gene. *Development* **136**, 61–71.
- Estella, C., McKay, D.J., and Mann, R.S. (2008). Molecular integration of wingless, decapentaplegic, and autoregulatory inputs into *Distalless* during *Drosophila* leg development. *Dev. Cell* **14**, 86–96.
- Estella, C., Voutev, R., and Mann, R.S. (2012). A dynamic network of morphogens and transcription factors patterns the fly leg. *Curr. Top. Dev. Biol.* **98**, 173–198.
- Whiteley, M., Noguchi, P.D., Sensabaugh, S.M., Odenwald, W.F., and Kassis, J.A. (1992). The *Drosophila* gene *escargot* encodes a zinc finger motif found in snail-related genes. *Mech. Dev.* **36**, 117–127.
- Hayashi, S., Hirose, S., Metcalfe, T., and Shiras, A.D. (1993). Control of imaginal cell development by the *escargot* gene of *Drosophila*. *Development* **118**, 105–115.
- Alberga, A., Boulay, J.L., Kempe, E., Dennefeld, C., and Haenlin, M. (1991). The snail gene required for mesoderm formation in *Drosophila* is expressed dynamically in derivatives of all three germ layers. *Development* **111**, 983–992.
- Fuse, N., Hirose, S., and Hayashi, S. (1996). Determination of wing cell fate by the *escargot* and snail genes in *Drosophila*. *Development* **122**, 1059–1067.
- Williams, J.A., Bell, J.B., and Carroll, S.B. (1991). Control of *Drosophila* wing and haltere development by the nuclear *vestigial* gene product. *Genes Dev.* **5** (12B), 2481–2495.
- Carroll, S.B., Weatherbee, S.D., and Langeland, J.A. (1995). Homeotic genes and the regulation and evolution of insect wing number. *Nature* **375**, 58–61.
- Ip, Y.T., Park, R.E., Kosman, D., Yazdanbakhsh, K., and Levine, M. (1992). *dorsal-twist* interactions establish snail expression in the presumptive mesoderm of the *Drosophila* embryo. *Genes Dev.* **6**, 1518–1530.
- Ip, Y.T., Levine, M., and Bier, E. (1994). Neurogenic expression of snail is controlled by separable CNS and PNS promoter elements. *Development* **120**, 199–207.
- Dunipace, L., Ozdemir, A., and Stathopoulos, A. (2011). Complex interactions between cis-regulatory modules in native conformation are critical for *Drosophila* snail expression. *Development* **138**, 4075–4084.
- Wieschaus, E., and Gehring, W. (1976). Clonal analysis of primordial disc cells in the early embryo of *Drosophila melanogaster*. *Dev. Biol.* **50**, 249–263.
- Córdoba, S., Requena, D., Jory, A., Saiz, A., and Estella, C. (2016). The evolutionarily conserved transcription factor Sp1 controls appendage growth through Notch signaling. *Development* **143**, 3623–3631.
- Estella, C., and Mann, R.S. (2010). Non-redundant selector and growth-promoting functions of two sister genes, *buttonhead* and *Sp1*, in *Drosophila* leg development. *PLoS Genet.* **6**, e1001001.
- Estella, C., Rieckhof, G., Calleja, M., and Morata, G. (2003). The role of *buttonhead* and *Sp1* in the development of the ventral imaginal discs of *Drosophila*. *Development* **130**, 5929–5941.
- Goto, S., and Hayashi, S. (1997). Specification of the embryonic limb primordium by graded activity of Decapentaplegic. *Development* **124**, 125–132.
- Kubota, K., Goto, S., Eto, K., and Hayashi, S. (2000). EGF receptor attenuates Dpp signaling and helps to distinguish the wing and leg cell fates in *Drosophila*. *Development* **127**, 3769–3776.
- Kubota, K., Goto, S., and Hayashi, S. (2003). The role of Wg signaling in the patterning of embryonic leg primordium in *Drosophila*. *Dev. Biol.* **257**, 117–126.

40. Reim, I., Lee, H.H., and Frasch, M. (2003). The T-box-encoding *Dorsocross* genes function in amnioserosa development and the patterning of the dorsolateral germ band downstream of Dpp. *Development* *130*, 3187–3204.
41. Hamaguchi, T., Yabe, S., Uchiyama, H., and Murakami, R. (2004). *Drosophila* Tbx6-related gene, *Dorsocross*, mediates high levels of Dpp and Scw signal required for the development of amnioserosa and wing disc primordium. *Dev. Biol.* *265*, 355–368.
42. Gebelein, B., Culi, J., Ryoo, H.D., Zhang, W., and Mann, R.S. (2002). Specificity of *Distalless* repression and limb primordia development by abdominal Hox proteins. *Dev. Cell* *3*, 487–498.
43. Gebelein, B., McKay, D.J., and Mann, R.S. (2004). Direct integration of *Hox* and segmentation gene inputs during *Drosophila* development. *Nature* *431*, 653–659.
44. Duncan, I.W. (2002). Transvection effects in *Drosophila*. *Annu. Rev. Genet.* *36*, 521–556.
45. Uhl, J.D., Zandvakili, A., and Gebelein, B. (2016). A Hox transcription factor collective binds a highly conserved *Distal-less* cis-regulatory module to generate robust transcriptional outcomes. *PLoS Genet.* *12*, e1005981.
46. Hannibal, R.L., Price, A.L., Parchem, R.J., and Patel, N.H. (2012). Analysis of *snail* genes in the crustacean *Parhyale hawaiiensis*: insight into *snail* gene family evolution. *Dev. Genes Evol.* *222*, 139–151.
47. Struhl, G., and Basler, K. (1993). Organizing activity of wingless protein in *Drosophila*. *Cell* *72*, 527–540.
48. Pfeiffer, B.D., Jenett, A., Hammonds, A.S., Ngo, T.T., Misra, S., Murphy, C., Scully, A., Carlson, J.W., Wan, K.H., Lavery, T.R., et al. (2008). Tools for neuroanatomy and neurogenetics in *Drosophila*. *Proc. Natl. Acad. Sci. USA* *105*, 9715–9720.
49. Sosinsky, A., Bonin, C.P., Mann, R.S., and Honig, B. (2003). Target Explorer: an automated tool for the identification of new target genes for a specified set of transcription factors. *Nucleic Acids Res.* *31*, 3589–3592.

STAR★METHODS

KEY RESOURCES TABLE

REAGENT or RESOURCE	SOURCE	IDENTIFIER
Antibodies		
Rabbit anti- β -Gal	MP	Cat# 559761; RRID: AB_2687418
Mouse anti- β -Gal	Promega	Cat# Z378A; RRID: AB_2313752
Rabbit anti-GFP	Thermo Fisher	Cat# A-6455; RRID: AB_221570
Mouse anti-Wg	DSHB	Cat# 4d4; RRID: AB_528512
Mouse anti-En	DSHB	Cat# 4D9; RRID: AB_528224
Mouse anti-Scr	DSHB	Cat# 6H4.1; RRID: AB_528462
Mouse anti-Ubx	DSHB	Cat# FP3.38; RRID: AB_10805300
Mouse anti-Antp	DSHB	Cat# 4C3; RRID: AB_528082
Rabbit anti-Abd-A	Santa Cruz	Cat# sc-98261; RRID: AB_1563449
Guinea Pig-anti-Sna	gift from Yutaka Nibu, Cornell University, USA	N/A
Rabbit anti-Vg	gift of Sean Carroll University of Wisconsin-Madison, USA	N/A
Guinea Pig anti-Dll	[19]	N/A
Guinea Pig anti-Hth	[19]	N/A
Rabbit anti-Doc-2	gift from Inhof Reim, Friedrich- Alexander University Erlangen- Nürnberg, Germany	N/A
Rabbit anti-Phospho-p44/42 MAPK	Cell Signaling	Cat# 9101; RRID: AB_331646
Experimental Models: Organisms/Strains		
<i>prd-Gal4</i>	FlyBase	FBtp0000358
<i>esg^{NP5130}-Gal4</i>	FlyBase	FBal0098823
<i>Dll^{MD23}-Gal4</i>	FlyBase	FBti0002783
<i>Doc-1-Gal4</i> (GMR 45H05)	FlyBase	FBsf0000164776
<i>Dll304-Gal4</i>	FlyBase	FBal0288749
<i>esg⁰⁵⁷³⁰-lacZ</i>	FlyBase	FBti0008070
<i>dpp¹⁰⁶³⁸-lacZ</i>	FlyBase	FBti0002737
<i>act5C>stop>lacZ; UAS-flp</i>	[46]	N/A
<i>Scr⁴</i>	FlyBase	FBal0015280
<i>Antp²⁵</i>	FlyBase	FBal0000566
<i>Ubx¹</i>	FlyBase	FBal0017338
<i>Ubx^{Mx12}abd-A^{M1}</i>	Gift from Ernesto Sanchez-Herrero	N/A
<i>Df(btd,Sp1)</i>	FlyBase	FBab0047246
<i>EGFR^{null}</i>	FlyBase	FBal0066102
<i>Df(3l)DocA</i>	FlyBase	FBab0037663
<i>tkv^{a12}</i>	FlyBase	FBal0016821

(Continued on next page)

Continued

REAGENT or RESOURCE	SOURCE	IDENTIFIER
<i>vg^{null}</i>	FlyBase	FBal0093753
<i>sna^{V2}</i>	FlyBase	FBal0015896
UAS- <i>rpr</i>	FlyBase	FBst0005823
UAS- <i>hid</i>	FlyBase	FBtp0012437
UAS-GFP	FlyBase	FBti0012493
UAS-TCF ^{DN}	FlyBase	FBtp0001721
UAS- <i>arm*</i> (delta N)	FlyBase	FBtp0001725
UAS- <i>brk</i>	FlyBase	FBtp0085350
UAS- <i>tkv^{QD}</i>	FlyBase	FBtp0001199
UAS- <i>Doc-2</i>	FlyBase	FBtp0017741
UAS-EGFR λ <i>top4.2</i>	FlyBase	FBtp0008722
UAS- <i>Scr</i>	FlyBase	FBtp0000719
UAS- <i>Antp</i>	FlyBase	FBtp0014554
UAS- <i>Ubx</i>	FlyBase	FBal0039098
UAS- <i>abd-A</i>	FlyBase	FBtp0085557
UAS- <i>Abd-B</i>	FlyBase	FBal0038086
UAS- <i>vg</i>	FlyBase	FBtp0051400
UAS- <i>sna</i>	FlyBase	FBtp0009053
Recombinant Proteins		
His-tag HM (Hth)	[40]	N/A
His-tag Exd	[40]	N/A
His-tag Dfd	[40]	N/A
His-tag Antp	[40]	N/A
His-tag Ubx	[40]	N/A
His-tag Abd-A	[40]	N/A
Oligonucleotides		
<i>sna</i> -DP sense: cagtAAGCTTgtggagcgcaccccaaagct	N/A	N/A
<i>sna</i> -DP asense: cagtAGATCTaaggatctgataaagaacgatctcc	N/A	N/A
<i>sna</i> -1.7 sense: cagtAAGCTTggttgggttaaagtagagcgc	N/A	N/A
<i>sna</i> -1.7 asense: cagtAGATCTtgcaaccgactaacaacgcatc	N/A	N/A
<i>sna</i> -1.7-1 sense: cagtAAGCTTggttgggttaaagtagagc	N/A	N/A
<i>sna</i> -1.7-1 asense: cagtAGATCTtgatctgctggtaagccc	N/A	N/A
<i>sna</i> -1.7-2 sense: cagtAAGCTTtcttatgggcttaccgca	N/A	N/A
<i>sna</i> -1.7-2 asense: cagtAGATCTcaaagctcagcagcggcagc	N/A	N/A
<i>sna</i> -1.7-3 sense: cagtAAGCTTgctgccgctgctgagctttg	N/A	N/A
<i>sna</i> -1.7-3 asense: cagtAGATCTatacgtagcattgctatc	N/A	N/A
<i>sna</i> -1.7-4 sense: cagtAAGCTTtagcaatgcctaacgtatcg	N/A	N/A
<i>sna</i> -1.7-4 asense: cagtAGATCTtgcaaccgactaacaacgc	N/A	N/A
<i>sna</i> -1.7-2A sense: cagtAAGCTTtcttatgggcttaccgca	N/A	N/A
<i>sna</i> -1.7-2A asense: cagtAGATCTggttaggaataaaccggaggag	N/A	N/A
<i>sna</i> -1.7-2B sense: cagtAAGCTTgaatggcgcgccctcgatt	N/A	N/A
<i>sna</i> -1.7-2B asense: cagtAGATCTcaaagctcagcagcggcagc	N/A	N/A
<i>sna</i> -1.7 sense pEntry: CACCggttgggttaaagtagagcgc	N/A	N/A
<i>sna</i> -1.7-2 sense pEntry: CACCtcttatgggcttaccgca	N/A	N/A
<i>sna</i> -1.7-3 sense pEntry: CACCgctgccgctgctgagctttg	N/A	N/A
Mad-1 sense: gtcgcaatcattaaacgatATCATAAgtTAATtatgtttacagattgtcg	N/A	N/A
Mad-1 asense: cgacaaatctgtaaacataATTAacaTTATGATatcgtttaagcggac	N/A	N/A
Mad-2 sense: ccggtttattcctaccgaaTTATAAATTTcgtatttaccctc	N/A	N/A

(Continued on next page)

Continued

REAGENT or RESOURCE	SOURCE	IDENTIFIER
Mad-2 asense: gaaggtataaaaaatcgaAAATTTATAAattcgtaggaataaacccg	N/A	N/A
Mad-3 sense: ccttatctatcggaccggctTAAGTAAATAAgtgtgtctgtcccatatctttcagg	N/A	N/A
Mad-3 asense: cctgaaagatatggggacagacagacaTTATTTACTTAagaccgggtccgatagataagg	N/A	N/A
Hox-1 Δ2 sense: agatttacgacagcatttcaCCCCttatgtcacattctagg	N/A	N/A
Hox-1 Δ2 asense: ccctagaatgtgacataaGGGGtgaaatgtgtcgtaaatct	N/A	N/A
Hox-2 sense: gcgcatctccgccgtaaacGTCGTACGttttatgtaatgcaac	N/A	N/A
Hox-2 asense: gttgcattaacataaaaCGTGACGACggtttacggcggagatgccc	N/A	N/A
Hox-3 sense: tgatctgcatgacccaagCGGGCATCAagcatttcataatattgtc	N/A	N/A
Hox-3 asense: gacataaattatgaaatgtGTATGCCCCgcttggtgcatcgagatca	N/A	N/A
Hox-4 sense: ggctaagcgcctctccTACTGCCCAAGGatgacattttatgtaatgc	N/A	N/A
Hox-4 asense: gcattaacataaaaatgtcatCCTTGGGCAGTAggagatgctgtagcc	N/A	N/A
Hox-5 sense: gggccatttaattgtctcgaCGTCCGGTAGTAcgctgctgagctttg	N/A	N/A
Hox-5 asense: caaagctcagcagcgtACTACCGGACGtcgagacaattaatggccc	N/A	N/A
Hox-6 sense: cgaaccatttgaaaataccccgccCGCCGGCGTTGccccgctctattcagttgcaaa	N/A	N/A
Hox-6 asense: tttgaactgaatgagcggggcGAACGCCGGCGggcgggggtatttcaaatggttcg	N/A	N/A
Recombinant DNA		
attB-hs43-nuc-lacZ	[19]	N/A
pBPGUw (Gal4)	[47]	N/A
Software and Algorithms		
ImageJ	https://imagej.nih.gov/ij/	N/A
JASPAR	http://jaspar.genereg.net/	N/A
Target Explorer	http://te.cryst.bbk.ac.uk/ [48]	N/A
Vienna <i>Drosophila</i> Resource Center	http://enhancers.starklab.org/	N/A

CONTACT FOR REAGENTS AND RESOURCE SHARING

Further information and requests for resources and reagents should be directed to and will be fulfilled by the Lead Contact, Carlos Estella (cestella@cbm.csic.es).

EXPERIMENTAL MODEL AND SUBJECT DETAILS

Fly and embryo culture

Drosophila melanogaster were maintained at 25°C on standard cornmeal agar diet in a humidified incubator. Embryos were collected in apple juice agar plates for 12 hr. Fly strains are provided in the [Key Resources Table](#).

Fly stocks

prd-Gal4, *esg*^{NP5130}-*Gal4*, *Dll*^{MD23}-*Gal4*, *Dll304-Gal4*, *tubGal80^{ts}*, *Doc-1-Gal4* (GMR 45H05), *esg*⁰⁵⁷³⁰-*lacZ* and *dpp*¹⁰⁶³⁸-*lacZ* are all described in FlyBase and key resource table. For lineage trace analyses the *act5C>stop>lacZ*; *UAS-flp* [47] stock was crossed with the corresponding *Gal4* lines. For *Dll* lineage analysis, we restricted the activity of the *Dll*^{MD23}-*Gal4* line to embryogenesis using the *tubGal80^{ts}*. Briefly, embryos were collected at 25° for 12hrs, transferred to 29° for 24hrs and then to 17° until dissection to shutdown Gal4 activity.

*Scr*⁴, *Antp*²⁵, *Ubx*^{Mx12}-*abd-A*^{M1}, *Df(btd,Sp1)*, *Df(3l)DocA*, *EGFR*^{null}, *tkv*^{a12}, *Dll*^{SA1}, *vg*^{null} and *sna*^{V2} are described in FlyBase. *UAS-hid*, *UAS-rpr*, *UAS-GFP*, *20XUAS-6XGFP*, *UAS-TCF^{DN}*, *UAS-arm** (delta N), *UAS-brk*, *UAS-tkv^{QD}*, *UAS-TCF^{DN}*, *UAS-Doc-2*, *UAS-EGFR*;*top4.2*, *UAS-Scr*, *UAS-Antp*, *UAS-Ubx*, *UAS-abd-A*, *UAS-Abd-B*, *UAS-vg*, *UAS-sna* are described in FlyBase and the [Key Resources Table](#).

METHOD DETAILS

Immunofluorescence

Imaginal discs were dissected in PBS and fixed with 4% paraformaldehyde in PBS for 25 min at room temperature. They were blocked in PBS, 1% BSA, 0.3% Triton for 1 hr, incubated with the primary antibody over night at 4°C, washed four times in blocking buffer, and incubated with the appropriate fluorescent secondary antibody for 1 hr at room temperature in the dark. They were then washed and mounted in Vectashield (Vector Laboratories). Embryos were collected every 12 hr and dechorionated in 100% bleach for 3 min and fixed in 1X PBS, 4% formaldehyde and heptane solution for 25 min. Then embryos were devitellinized with methanol and washed in PBT (1X PBS and 0.1% tween 20). Embryos were blocked in 3% BSA PBT for 1 hr and incubated with primary antibodies over night, washed four times in PBT, and incubated with the appropriate fluorescent secondary antibody for 1 hr at room temperature in the dark. They were then washed and mounted in Vectashield.

Confocal images were obtained with a Zeiss LSM510 coupled to a vertical Axio Imager.Z1 M. For visualization, a Z-projection was generated using ImageJ (<https://imagej.nih.gov/ij/>) for representative embryos of each stage and genotype.

Generation of transgenes

sna-DP, *sna*-1.7, *sna*-1.7-1, *sna*-1.7-2, *sna*-1.7-3 and *sna*-1.7-4 sequences were cloned into the attB-hs43-nuc-lacZ plasmid vector [22]. *sna*-1.7 and *sna*-1.7-3 were also cloned in the pBPGUw (Gal4) vector [48]. The primers used for cloning each reporter line are described in the [Key Resources Table](#).

Putative Mad and Hox binding sites were identified on the basis of a bioinformatics analysis combining data from the JASPAR CORE Insecta database (<http://jaspar.genereg.net/>) and the Target Explorer tool [49]. Mutagenesis of the Mad and Hox putative binding sites was performed using the QuikChange Site-Directed Mutagenesis Kit (Stratagene). The primers used for the mutagenesis are described in the key resources table. All reporter constructs were inserted in the same site 3R (86Fb) to allow proper comparisons. In addition, *sna*-DP-*lacZ* and *sna*-1.7-*Gal4* were also inserted in 2R (51D).

Electrophoretic mobility shift assays (EMSAs)

Binding experiments were performed as described previously [42]. Proteins were expressed as His-tag fusions and purified from BL21 cells. HM protein (HM refer to the full-length homeodomainless isoform of Hth) was purified in complex with Exd. Binding reactions for Dfd, Ubx, and AbdA were performed with 150nM Hox protein and 75nM Exd/HM. Antp protein was used at a concentration of 75nM with 30nM Exd/HM. DNA probes were radiolabeled with P32 and used at a concentration of 6nM in the binding reaction.

QUANTIFICATION AND STATISTICAL ANALYSIS

sna-DP and Dll positive cells were counted by taking multiple Z stacks to encompass the entire primordia using ImageJ (<https://imagej.nih.gov/ij/>). At least 10 embryos were counted per genotype. Statistical analysis, * $p < 0.05$ by Student's t test. Error bars represent SEM.